Electrosprayed core-shell nanoparticles of PVP and shellac for furnishing biphasic controlled release of ferulic acid

Lei Cui
Zhe-Peng Liu
Deng-Guang Yu
Shu-Ping Zhang
S. W. Annie Bligh
Na Zhao

This is an author's accepted manuscript of an article published in Colloid and Polymer Science, 292 (9), pp. 2089-2096, September 2014.

The final publication is available at Springer via
http://dx.doi.org/10.1007/s00396-014-3226-8

Electrosprayed core-shell nanopartciles of PVP and shellac for furnishing biphasic controlled release of ferulic acid

Lei Cui [1,*], Zhe-Peng Liu [2], Deng-GuangYu[3,*] Shu-Ping Zhang [1], SW Annie Bligh [4], Na Zhao[3]

[1] Tin Ka Ping College of Science, University of Shanghai for Science and Technology, 516 Jungong Road, Shanghai 200093, China

[2] School of Medical Instrument and Food Engineering, University of Shanghai for Science and Technology, 516 Jungong Road, Shanghai 200093, China

[3] School of Materials Science & Engineering, University of Shanghai for Science and Technology, 516 Jungong Road,Shanghai 200093, P. R. China

[4] Department of Complementary Medicine, School of Life Sciences, University of Westminster, 115 New Cavendish Street, London W1W 6UW.

Running Head: Biphasic release PVP-shellac nanoparticles

Corresponding author:
Dr. Lei Cui and Dr. Deng-Guang Yu

Address:
Tin Ka Ping College of Science,
University of Shanghai for Science and Technology,
516 Jungong Road,
Yangpu District,
Shanghai 200093, P.R. China
Tel: +86-21-55274069
Fax: +86-21-55270632
Email: ydg017@gmail.com (DG Yu); cuilei15@usst.edu.cn (L Cui)

Abstract Coaxial electrospraying was explored to organize polymer excipients in a core-shell manner for providing biphasic controlled release of active ingredient. With ferulic acid (FA) as a model drug, and shellac and polyvinylpyrrolidone as the core and shell polymeric matrices, core-shell nanoparticles were successfully fabricated. A series of tests were carried out to characterize the prepared core-shell nanoparticles and also the nanoparticles prepared using a single fluid electrospraying of the shell or core fluids alone. The core-shell nanoparticles had an average diameter of 530 ± 80 nm with clear core-shell structure. The contained FA was converted to an amorphous state both in the core and the shell parts due to the favorable hydrogen bonding between the components. In vitro dissolution tests demonstrated that the core-shell nanoparticles were able to provide the desired biphasic drug controlled release profiles. Coaxial electrospraying is a useful tool for the development of novel nano drug delivery systems from polymers.

Keywords Coaxial electrospraying; Core-shell nanopartciles; Shellac; Bipahsic controlled release; Structural nanocomposites

Introduction

Nanosizing strategies have exerted great influence on the development of novel drug delivery systems (DDS) [1,2]. Today, as the progress of nanotechnology, more and more attention has been paid to the fabrication of nanostructures, by which improved or even new functional performances can be achieved [3]. One of the most popular and simple nanostructures is the core-shell structure (with different exterior and interior) [4], and many complicated structures are essentially the derivatives of this structure, such as making holes in the shell or encapsulating even smaller nanoparticles in the core.

Because of the usefulness of this structure in tailoring the functions of the products, a wide variety of methods have been reported for the fabrication of core-shell products, such as core-sheath nanofibers and core-shell nanoparticles [5, 6]. It is a common sense that the bottom-up approaches are more suitable than top-down approaches for the synthesis of core-shell nanostructures [7]. However, coaxial electrohydrodynamic atomization processes (EHDA, including electrospinning, electrospraying and e-jet printing) have successfully been used to generate core-shell nanostructures in a top-down manner, for instance in the preparation of core-sheath nanofibers by electrospinning [8, 9]. Compared with some bottom-up chemical methods which are often multiple-step, time-consuming, coaxial electrospraying is able to generate core-shell nanoparticles in a single step and straightforwardly [10].

Based on the fact that liquids can readily interact with electrical energy, EHDA processes are developed for preparing nano products through the fast removing of organic solvents employing electrical energy directly [11-13]. The fast drying electrospinning process not only can propagate the physical state of the components in the liquid solutions into the solid nanofibers, but also can duplicate the concentric structure of the spinneret on a macroscale to products on a nanoscale. Thus, the components in the sheath and core fluids often occur in the sheath and core parts of the nanofibers, respectively, with little diffusion [14]. Similarly, coaxial electrospraying has been proved to be a powerful tool for generating core-shell micro-/nano-particles, and also hollow microspheres from the concentric fluids based on the templates of a concentric spray head [15-17].

Biphasic drug controlled release is a special release type that obeys biological rhythm for safe and effective drug delivery and convenient administration [18]. An initial rapid release of a fraction of the dose after administration is in favor of relieving the symptoms of the disease, and

later a sustained release of the remaining dose over a defined period can optimize the therapy and avoid repeated administration for the patients' convenience [19]. Many traditional pharmaceutical methods and also the emerged advanced techniques have been exploited in literature to produce novel materials or DDS for furnishing biphasic release, taking its advantage in a more accurate time-programmed administration of active ingredients and fulfilling the specific therapeutic needs of some diseases. [20].

Over the past several decades, polymer science has acted as the backbone for supporting the development of pharmaceutics, particularly in the area of controlled release [21]. Because of their relative abundance, low cost, and bio-degradable and eco-friendly profiles, natural polymeric materials has drawn increasing attention and interest as potential pharmaceutical excipients [22]. Shellac is the purified product of the natural material Lac which is secreted by the small parasitic insect *Kerria Lacca* on various host trees in South Eastern Asia. It has properties of water resistance, biocompatibility and fine membrane forming ability. Shellac has found its applications in agriculture, food products, and DDS as the only pharmaceutically used resin of animal origin [23]. The dissolution behavior of shellac may be of interest for sustained release or colon targeting applications, particularly in the drug formations of traditional coating way [24].

Building on the above-mentioned knowledge, this study investigated the preparation of drug-loaded core-shell nanoparticles using a coaxial electrospraying process for providing a biphasic drug controlled release profile. Shellac and polyvinylpyrrolidone (PVP) were exploited as the core and shell polymeric matrices, respectively. PVP has a wide variety of applications in pharmaceutics, medicine and cosmetics [25,26]. Ferulic acid (FA), 4-hydroxy-3-methoxycinnamic acid, was explored as a drug model. It is an antioxidant that is able to neutralize free radicals

(superoxide, nitric oxide and hydroxyl radical), which can cause oxidative damage to cell membranes and DNA. Studies have shown that FA can decrease blood glucose levels and so could be applicable for the treatment of diabetes patients and it can also reduce the risk of many cancers, including cancer of the stomach, breast, colon, liver, prostate, lung and tongue [27, 28].

Experimental

Materials FA was purchased from Shanghai Winherb Medical Sci & Tech Development Co., Ltd (Shanghai, China). PVP K25 (M_w = 30,000) was purchased from the Sigma-Aldrich Co. Ltd. (Shanghai, China). Shellac (purity of 95%, wax free) was supplied by the ShengHui Agricultural science and Technology Co., Ltd. (Yunnan, China). Sodium hydrate, hydrochloric acid and anhydrous ethanol were provided by the Shanghai Shiyi Chemical Reagent Co., Ltd. (Shanghai, China). All chemicals used were analytical grade. Water was double distilled just before use.

Coaxial electrospraying A mixed solution of 5% (w/v) PVP and 1% (w/v) FA in ethanol was prepared as the shell fluid. The core solution consisted of 10% (w/v) shellac and 1% (w/v) FA in ethanol. A homemade concentric spinneret was used to carry out coaxial electrospraying. Two syringe pumps (KDS 100 and KDS 200, Cole-Parmer, Vernon Hills, IL, USA) were employed to drive the shell and core fluids. A high voltage supply (ZGF 60kV / 2 mA, Shanghai Sute Electrical Co., Ltd, Shanghai, China) provided an applied voltage below 60 kV. All electrospraying processes were carried out under ambient conditions (27 °C ± 2 °C with relative humidity 51% ± 7%). The resultant nanoparticles were collected on a metal collector wrapped with aluminum foil at a fixed distance of 10 cm from the needle tip of the spray head. Experiments were recorded using a digital video recorder (PowerShot A640, Canon, Japan) under 11 × magnifications. The nanoparticles were stored in a desiccator before characterization was undertaken. Details of the

parameters for electrospraying and the resultant products are listed in Table 1.

Characterization

Morphology and structure The morphologies of the core-shell nanoparticles were assessed using an S-4800 field emission scanning electron microscope (FESEM, Hitachi, Tokyo, Japan). Their average sizes were determined by measuring the diameters of more than 100 particles in FESEM images using the Image J software (National Institutes of Health, Bethesda, MD, USA). The topographies of raw PVP and FA were observed under cross-polarized light using an XP-700 polarized optical microscope (Shanghai Changfang Optical Instrument Co. Ltd, Shanghai, China) and crude shellac was observed using the PowerShot A640 digital video recorder. Transmission electron microscopy (TEM) images of nanoparticles N3 were taken on a JEM 2100F field-emission transmission electron microscope (JEOL, Tokyo, Japan). TEM samples were prepared by fixing a lacey carbon coated copper grid on the metal collector and nanoparticles sprayed directly onto the grid.

Physical status of the components X-ray diffraction (XRD) was performed on a D/Max-BR diffractometer (RigaKu, Tokyo, Japan) over the 2θ range of 5–60° using Cu Kα radiation at 40 mV and 30 mA. Attenuated total reflectance Fourier transform infrared (ATR-FTIR) spectra were recorded on a Nicolet-Nexus 670 FTIR spectrometer (Nicolet Instrument Corporation, Madison, WI, USA) over the range 500-4000 cm^{-1} and at a resolution of 2 cm^{-1}. Approximately 5 mg of the materials were placed directly on the diamond window for spectra acquisition.

In vitro dissolution *In vitro* dissolution tests were carried out according to the Chinese Pharmacopoeia (2010 Ed.). Dissolution studies were undertaken following Method II, a paddle method, using a RCZ-8A apparatus (Tianjin University Radio Factory, Tianjin, China). 200 mg

samples of N1, N2 and N3 were first placed in 600 mL of 0.01N HCl for 2 h, and later 0.24 g sodium hydrate was added to the dissolution medium to adjust its pH value to 7.0. The temperature of the dissolution medium was fixed at 37 ± 1 °C and the instrument was set to stir at 50 rpm. At predetermined time points, aliquots of 5.0 mL were withdrawn from the dissolution medium and replaced with fresh medium to maintain a constant volume. After filtration through a 0.22 μm membrane (Millipore, MA, USA) and appropriate dilution with phosphate buffer (PBS, pH7.0, 0.1M), samples were analyzed at λ_{max} =322 nm using a UV–vis spectrophotometer (UV-2102PC, Unico Instrument Co. Ltd., Shanghai, China). The cumulative amount of FA released at each time point was back-calculated from the data obtained against a predetermined calibration curve. Experiments were carried out six times and results are reported as mean values ± S.D.

Results and discussion

Coaxial electrospraying A schematic diagram of the coaxial electrospraying process is shown in Fig. 1a. A typical electrospraying system consists of four major components: one or more syringe pumps, a power supply, a spray head and a collector, by which the electrical energy is directly exploited to dry and solidify micro-fluid jets, causing solvent evaporation and producing micro-/nano- size products effectively. During the electrospraying process, a liquid is fed to a metal capillary at the end of which a droplet is formed. When the droplet is exposed to a strong electrical field, a charge is induced on its surface. Provided the liquid has sufficient electrical conductivity, there will be a range of combinations of the liquid flow rate and the applied voltage for which the drop will assume a conical shape (the Taylor cone). At the apex of this cone, a narrow jet is formed (cone-jet mode) which subsequently breaks up into fine droplets (Fig. 1b).

Electrospraying first generates near-monodisperse droplets whose size can be varied between a few to hundreds of micrometers. Later, the droplets rapidly shrink due to the fast evaporation of solvents resulting from the Coulombic explosion. The huge surface areas of the micro-droplets provide the possibility for complete of the solvents and the solidification of products. The facile interactions of electrons with fluid solvents accelerate their evaporation [29]. The electrons always accumulate on the surface of droplets and result in the fast fission to bring a Coulombic explosion (i.e. atomization). Thus during the coaxial electrospraying processes, the outer shell fluids can dominate the splitting of droplets step-by-step, and by which the next level of droplets also have the core-shell structures until the formation of solid core-shell nanoparticles (Fig. 1b).

The arrangement of the apparatus used in this work is shown in Fig. 2a. The inset of Fig. 2a shows a digital picture of the home-made concentric spray head, which consists of two stainless steel capillaries, with the smaller one (27G, , the outer and inner diameters are 1.25 and 0.84, respectively) penetrated through the larger one (18G, the outer and inner diameters are 0.42 and 0.21, respectively) to form a concentric structure. The inner capillary projected a length of 0.2 mm out of the outer capillary for avoiding possible mixing. An alligator clip was used to connect the spray head with the power supply (Fig. 2b).

After some optimization, a fixed high voltage of 20 kV was applied. A typical coaxial electrospraying process was exhibited in Fig. 2c, which was taken under a same shell and core fluid flow rate of 0.2 mL/h. A short straight thinning jet is emitted from the compound Taylor cone (Fig. 2c and 2d) and is followed by the explosion atomization region. The core fluid showed dark brown color due to the dissolution of shellac and the shell fluid can be discerned by the visible inner capillary in Fig. 2d. The Taylor cone exhibited a triangle with straight line, while the Taylor

cone of the electrospinning always shows a camber line due to high surface tensions of electrospinnable solutions [19]. When one of the shell or core fluid flow rates was adjusted to 0 mL/h, then a single fluid electrospraying could be implemented for the preparation of nanoparticles N1 and N2.

Morphology and structure Single fluid electrospraying of the shell and core fluid alone resulted in solid products of the nanoparticles N1 and N2 (Table 1 and Fig. 3a and b). They have an average diameter of 470 ± 110 nm (Fig. 3a) and 720 ± 180 nm (Fig. 3b), respectively. With core and shell flow rates were controlled at 0.2 mL/h, the core-shell nanoparticles N3 were generated, which had an average diameter of 530 ± 80 nm (Fig. 3c and 3d). The insets of Fig. 3a, b and d showed that nanoparticles N2 and N3 were compact and spherical nanoparticles, whereas nanoparticles N1 were somewhat flat with depressions. All the three types of nanoparticles had a few satellites on the surface.

Fig. 4 shows the TEM images of the coaxial electrosprayed nanoparticles N3. They have clear core-shell structures, with the cores a darker gray color because of the presence of shellac. There is uniform gray shading in both the shell and core parts of the microparticles in all the images, indicating that FA is uniformly distributed in the PVP matrix of the shell part, and also in the shellac matrix of the core part. The satellites had a similar gray level of the shell part, suggesting that they were fabricated by the fission of the shell fluid during the coaxial electrospraying process.

Physical status and compability

The crude FA exists as crystalline materials, which is demonstrated by the observation of colorful images when their particles are viewed under polarized light (Fig. 5a). In contrast to the

observations of FA under polarized light, the images of PVP powders show no bright colors, suggesting it is amorphous (Fig. 5b). Shellac exists as reddish-brown platelets, as shown by the digital picture in Fig. 5c. The physical status of the components and nanoparticles were further investigated using XRD. The presence of distinct peaks in the XRD patterns of the FA raw particles indicated that FA was present as crystalline material with characteristic diffraction peaks (Fig. 5d). No distinct peaks in the spectrum of PVP and shellac evidently indicated that the molecular orientation and arrangement of the polymers were disordered, i.e. an amorphous state. Similarly, there were no discrete peaks in the spectrum of nanoparticles N1, N2 and N3, which implied that the original crystalline FA was no longer present as crystalline material, but had been converted into an amorphous state, no matter it is in the core part or in the shell part (Fig. 5d). The solubility behavior of poorly water-soluble drugs is one of the most challenging aspects of the formulation development in pharmaceutics [30]. It is desirable if the process can alter the physical status of drug to the favorable nanocrystalline, amorphous or solid solution phases for effective drug delivery. Here, the coaxial electrospraying process exhibited its capability of generating amorphous structural nanomaterials of poorly water-soluble drug.

ATR-FTIR was conducted to investigate the compatibility between the active ingredients and the polymeric matrices in the nanoparticles. Compared to the spectra of pure FA and shellac, there are significant changes in the spectra of the nanoparticles (Fig. 6), including (1) the characteristic peaks of the carbonyl groups (C=O stretch vibration) at 1714 cm^{-1} in shellac spectra shifting to 1698 cm^{-1} in nanoparticles N2 and to 1702 cm^{-1} in Nanoparticles N3. Similarly, the characteristic peaks of the carbonyl groups (C=O stretch vibration) at 1660 cm^{-1} in PVP spectra shifting to 1654 cm^{-1} in nanoparticles N1, and 1656 cm^{-1} in Nanoparticles N3 ; (2) the decrease or even

disappearance of the numerous peaks in the finger region of FA in all the three types of nanoparticles; (3) the characteristic peaks of the carbonyl groups (C=O stretch vibration) at 1663 and 1689 cm-1 of FA melting into the 1654 cm^{-1} in nanoparticles N1, 1698 cm^{-1} in nanoparticles N2, and 1656 cm^{-1} and 1702 cm^{-1} in nanoparticles N3. All these changes can be attributed to hydrogen bonding between FA and shellac, and between FA and PVP, including (1) between C=O of FA and O-H of shellac, and (2) between the C=O of shellac/PVP and the O-H of FA, as clearly shown in the molecular formula (Fig. 6). All these secondary interactions would avail to the formation of FA-PVP nanocomposites in nanoparticles N1 and the shell part of nanoparticles N3, and the formation of FA-shellac nanocomposites in nanoparticles N2 and the core part of nanoparticles N3. Thus the nanoparticles were essentially a structural nanocomposite.

Functional performance and controlled-release mechanism The *in vitro* drug release profiles of the three nanoparticles are given in Fig. 7a and 7b. The nanoparticles N1 disappeared instantly when they were put into the acidic dissolution medium. *In vitro* dissolution tests verified that all the FA was dissolved into the bulk media in the first hour. This result is attributed to the hydrophilic properties of PVP, large surface areas of the nanoparticles, and the amorphous status of FA in the nanocomposites, which made the FA molecules can dissolve simultaneously with PVP molecules through erosion mechanism.

The nanoparticles N2 released only 1.7% of the incorporated FA during 1 h immersion in the acid dissolution medium. This resulted from the insolubility of shellac in low pH environments. After the dissolution environment was changed to a neutral condition, nanopartciles N2 released the embedded FA over around 9 h in a sustained manner. The nanoparticles N3 evidently exhibited a combination of the release profiles of nanoparticles N1 and N2 with the shell part providing an

initial rapid release and the core part furnishing a sustained release.

A suggested mechanism is put forward in Fig. 7c. Based on the different dissolution properties of the polymeric excipients, and intentional arrangement of them into the core-shell nanostructure, a structure-activity relationship at nanoscale can be achieved. The release of the encapsulated drug in the core-shell nanoparticles can be manipulated step-by-step through the gradual dissolutions of the layered polymer matrices in different environments. In the present biphasic release profiles provided by nanoparticles N3, 51.2% of the contained drug was freed during the first phase, and the remnant released in a sustained manner. Certainly, the release content in the two phases can be easily tuned simply through the adjustment of drug content in the shell or core fluids during the preparation of the core-shell nanoparticles. Further *in vivo* experiments will be conducted to investigate the medicinal effects of the nanoparticles N3.

Conclusions

Core-shell nanoparticles were successfully fabricated using a coaxial electrospraying process. FESEM and TEM images demonstrated that the core-shell nanoparticles had an average diameter of 530 ± 80 nm with clear core-shell structure. XRD and polarized microscopy showed that the contained FA was converted to an amorphous state both in the core and the shell parts due to the favorable hydrogen bonding between the components, as verified by the ATR-FTIR spectra. In vitro dissolution tests demonstrated that the core-shell nanoparticles could combine the drug release profiles provided by the nanoparticles prepared from the shell or core fluid alone through a single fluid electrospraying, providing the designed biphasic drug release profiles. Coaxial electrospraying is a powerful tool for generating core-shell nanostructures with tailored components and compositions, and thus to realize a structure-activity relationship at nanoscale.

Acknowledgements This work was supported by the National Science Foundation of China (Nos. 51373101 & 21202097), the Natural Science Foundation of Shanghai (No.13ZR1428900) and the Key Project of the Shanghai Municipal Education Commission (No.13ZZ113).

References

1. Farokhzad OC (2008) Nanotechnology for drug delivery: the perfect partnership. Expert Opin Drug Del 5:927–929
2. Hubbell JA, Chikoti A (2012) Nanomaterials for drug delivery. Science 337: 303-305
3. Webster TJ (2006) Nanomedicine: what's in a definition? Int J Nanomedicine 1:115-116
4. Liang X, Li J, Joo JB, Gutierrez A, Tillekarathe A, Lee I, Yin Y, Zaera F (2012) Diffusion through the shells of yolk–shell and core–shell nanostructures in the liquid phase. Angew Chem Int Ed 51: 8034-8036
5. Agarwal S, Greiner A, Wendorff JH (2013) Functional materials by electrospinning of polymers. Prog Polym Sci 38:963–991
6. Enayati M, Ahmad Z, Stride E, Edirisinghe M (2010) One step electrohydrodynamic production of drug-loaded micro- and nano-particles. J Roy Soc Interf 7:667-675
7. Chaudhuri RG, Paria S (2012) Core/shell nanoparticles: classes, properties, synthesis mechanisms, characterization, and applications. Chem Rev 112: 2373-2433
8. Moghe AK, Gupta BS (2008) Co-axial electrospinning for nanofiber structures: Preparation and applications. Polym Rev 48:353-377
9. Yu DG, Liao Y, Li X, Chian W, Li Y, Wang X (2013) Colon-targeted drug delivery core-sheath nanofibers prepared using a modified coaxial electrospinning. J Control Release 172:e14–e97
10. Loscertales IG, Barrero A, Guerrero I, Cortijo R, Marquez M, Canan-Calvo AM (2002) Micro/nano encapsulation via electrified coaxial liquid jets. Science 295:1695–1698
11. Nagy ZK, Balogh A, Drávavölgyi G, Ferguson J, Pataki H, Vajna B, Marosi G (2013) Solvent-free melt electrospinning for preparation of fast dissolving drug delivery system and comparison with solvent-based electrospun and melt extruded systems. J Pharm Sci 102:508–517
12. Li W, Yu DG, Chen K, Wang G, Williams GR (2013) Smooth preparation of ibuprofen/zein microcomposites using an epoxy-coated electrospraying head. Mater Lett 93:125-128
13. Nagy ZK, Wagner I, Suhajda Á, Tobak T, Harasztos AH, Vigh T, Sóti PL, Pataki H, Molnár K, Marosi G (2014) Nanofibrous solid dosage form of living bacteria prepared by electrospinning. eXPRESS Polym Lett 8:352–361
14. Yu DG, Wang X, Li XY, Chian W, Li Y, Liao YZ (2013) Electrospun biphasic drug release polyvinylpyrrolidone/ ethyl cellulose core/sheath nanofibers. Acta Biomater 9:5665-5672
15. Eltayeb M, Stride E, Edirisinghe M (2013) Electrosprayed core–shell polymer–lipid

nanoparticles for active component delivery. Nanotechnology 24:465604 (9pp)

16. Zhang Q, Wang L, Wei Z, Wang X, Long S, Yang J (2012) A new simple method to prepare hollow PES microspheres. Colloid Polym Sci 290:1257–1263

17. Zhang Q, Liu J, Wang X, Li M, Yang J (2010) Controlling internal nanostructures of porous microspheres prepared via electrospraying. Colloid Polym Sci 288:1385–1391

18. Song B, Wu C, Chang J (2012) Dual drug release from electrospun poly (lactic-co-glycolic acid)/mesoporous silica nanoparticles composite mats with distinct release profiles. Acta Biomater 8:1901-1907

19. Yu DG, Liu F, Cui L, Liu ZP, Wang X, Bligh SWA (2013) Coaxial electrospinning using a concentric Teflon spinneret to prepare biphasic-release nanofibers of helicid. RSC Adv 3:17775-17783

20. Yu DG, Williams GR, Wang X, Liu XK, Li HL, Bligh SWA (2013) Dual drug release nanocomposites prepared using a combination of electrospraying and electrospinning. RSC Adv 3:4652-4658

21. Krushnakumar J Gandhi, Subhash V Deshmane, Kailash R Biyani (2012) Polymers in pharmaceutical drug delivery system: A review. Int J Pharma Sci Rev Res 14:57-66

22. Ogaji IJ, Nep EI, Audu-Peter JD (2012) Advances in natural polymers as pharmaceutical excipients. Pharm Anal Acta 3:146

23. Limmatvapirat S, Panchapornpon D, Limmatvapirat C, Nunthanid J, Luangtana-Anan M, Puttipipatkhachorn S (2008) Formation of shellac succinate having improved enteric film properties through dry media reaction. Eur J Pharm Biopharm 70:335–344

24. Limmatvapirat S, Limmatvapirat C, Puttipipatkhachorn S, Nuntanid J, Luangtana-anan M (2007) Enhanced enteric properties and stability of shellac films through composite salts formation. Eur J Pharm Biopharm 67:690–698

25. Yu DG, White K, Yang JH, Wang X, Qian W, Li Y (2012) PVP nanofibers prepared using co-axial electrospinning with salt solution as sheath fluid. Mater Lett 67: 78-80

26. Vigh T, HorváthováT, Balogh A, Sóti PL, Drávavögyi G, Nagy ZK, Marosi G (2013) Polymer-free and polyvinylpirrolidone-based electrospun solid dosage forms for drug dissolution enhancement. Eur J Pharm Sci 49:595–602

27. Yang JM, Zha L, Yu DG, Liu J (2012) Coaxial electrospinning with acetic acid for preparing ferulic acid/zein composite fibers with improved drug release profiles. Colloid Surf B: Biointerf 102:737-743.

28. Anselmi C, Centini M, Maggiore M, Gaggelli N, Andreassi M, Buonocore A, Beretta G, Facino RM (2008) Permeation and distribution of ferulic acid and its α-cyclodextrin complex from different formulations in hairless rat skin. J Pharm Biomed Anal. 46 (2008) 645-652

29. Salata OV (2005) Tools of nanotechnology: Electrospray. Curr Nanosci 1: 25-33

30. Li XY, Li YC, Yu DG, Liao YZ, Wang X (2013) Fast disintegrating quercetin-loaded drug

delivery systems fabricated using coaxial electrospinning. Int J Mol Sci 14:21647-21659

Table and Figure Caption

Table 1 Parameters used for electrospraying and details of the nanoparticulate products

Fig. 1 Coaxial electrospraying: (a) a schematic diagram of the coaxial electrospraying process; (b) a diagram of the atomization mechanism

Fig. 2 Implementation of the coaxial electrospraying process. a) the arrangement of the apparatus used in this work (the inset Image is the nozzle of the concentric spray head); b) the connection of the spray head with the power supply using an alligator clip; c) a typical coaxial electrospraying process under an applied voltage of 20 kV, with a same shell and core fluid flow rates of 0.2 mL/h; d) the compound Taylor cone

Fig. 3 FESEM images of the nanoparticles, and their diameter distributions, (a) nanoparticles N1, (b) nanoparticles N2, (c) and (d) nanoparticles N3 with different magnifications

Fig. 4 TEM images of nanoparticles N3

Fig. 5 XRD patterns and observations of the crude particles. a) microscopy images viewed under cross-polarized light: a) FA; b) PVP; c) a digital image of shellac; d) XRD patterns of the starting materials and nanoparticles N1, N2 AND N3

Fig. 6 ATR-FTIR spectra of the raw materials and nanoparticles, and the molecular structures of PVP, FA and shellac

Fig. 7 *In vitro* dissolution tests. a) *in vitro* FA release profiles during the whole time period (n=6); b) *in vitro* FA release profiles of the first hour (n=6); c) a schematic about the drug controlled release mechanisms from the core-shell nanoparticles

Table 1 Parameters used for electrospraying and details of the nanoparticulate products

No.	Electrospraying process	Flow rate (mL/h)		Morphology	Diameter (nm)
		Shell fluid [a]	Core fluid [b]		
N1	Single fluid	0.4	--	Nanoparticles	470 ± 110
N2	Single fluid	--	0.4	Nanoparticles	720 ± 180
N3	Coaxial	0.2	0.2	Nanoparticles	530 ± 80

[a] The shell fluid consisted of 5% (w/v) PVP K25 and 1% (w/v) FA in ethanol.

[b] The core fluid consisted of 10% (w/v) shellac and 1% (w/v) FA in ethanol.

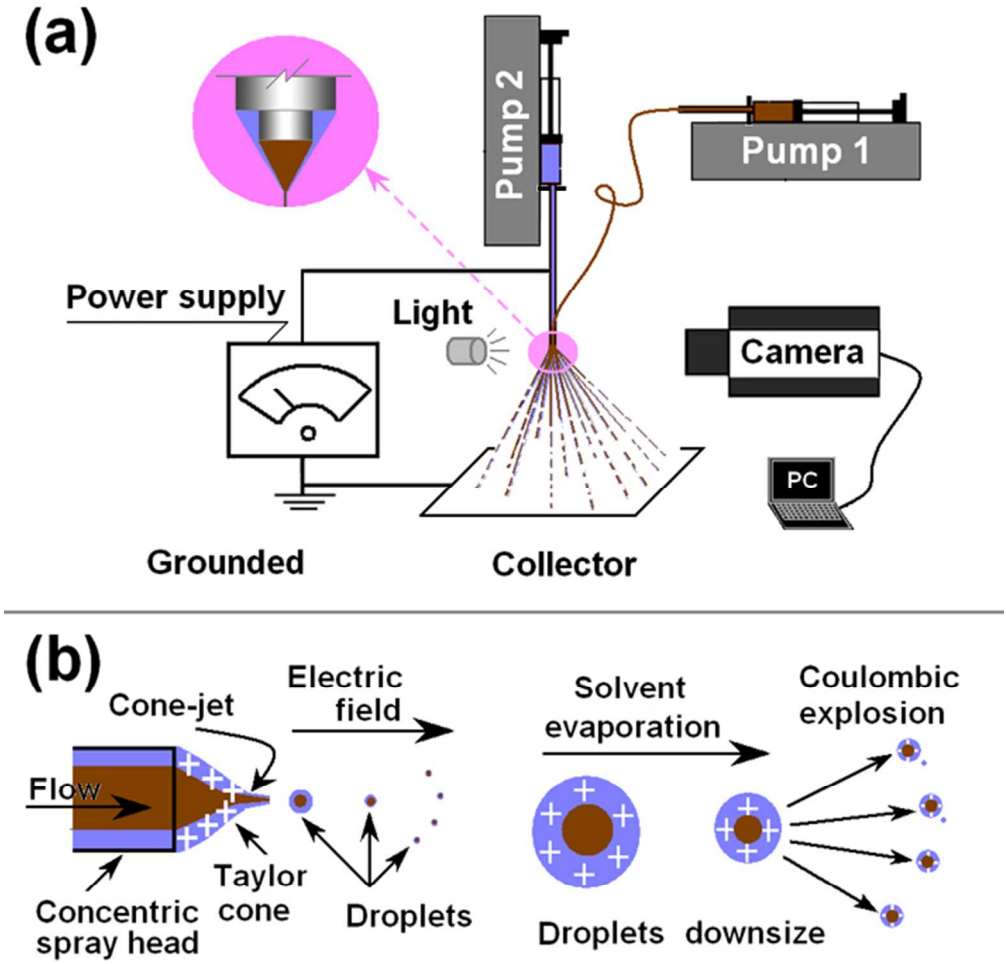

Fig. 1 Coaxial electrospraying: (a) a schematic diagram of the coaxial electrospraying process; (b) a diagram of the atomization mechanism
60x59mm (300 x 300 DPI)

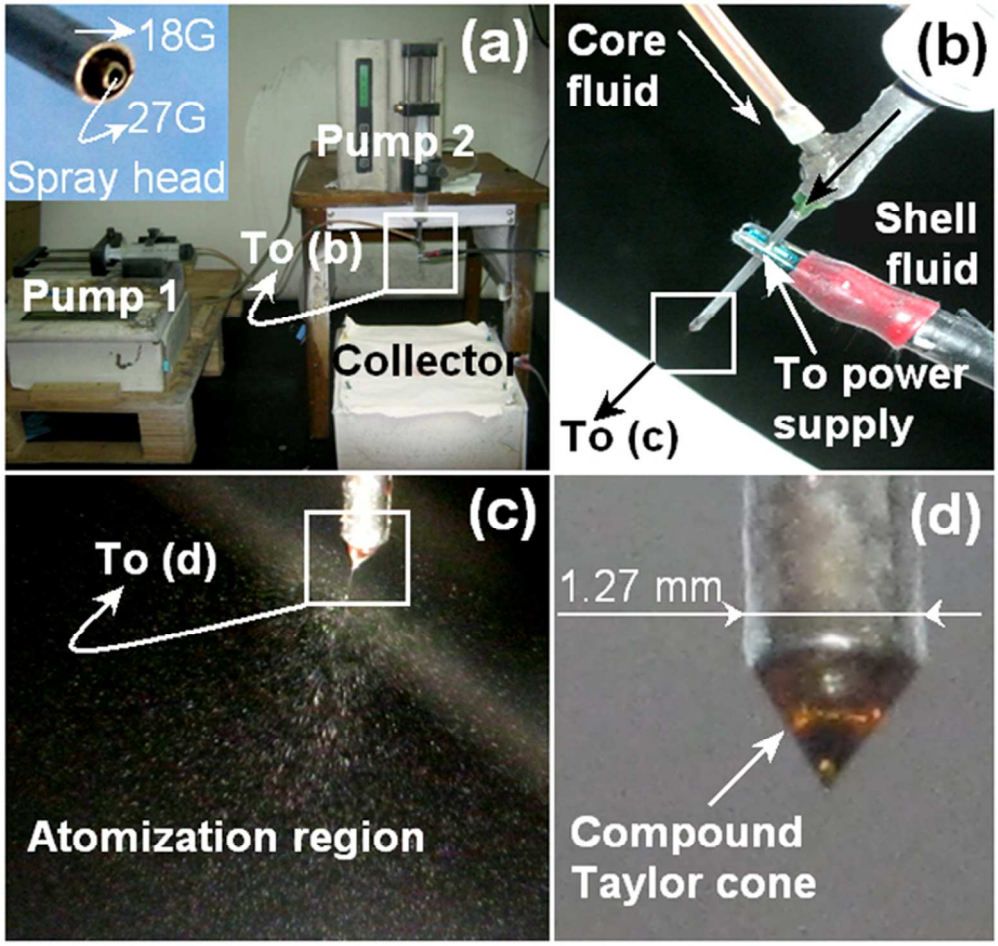

Fig. 2 Implementation of the coaxial electrospraying process. a) the arrangement of the apparatus used in this work (the inset Image is the nozzle of the concentric spray head); b) the connection of the spray head with the power supply using an alligator clip; c) a typical coaxial electrospraying process under an applied voltage of 20 kV, with a same shell and core fluid flow rates of 0.2 mL/h; d) the compound Taylor cone
60x56mm (300 x 300 DPI)

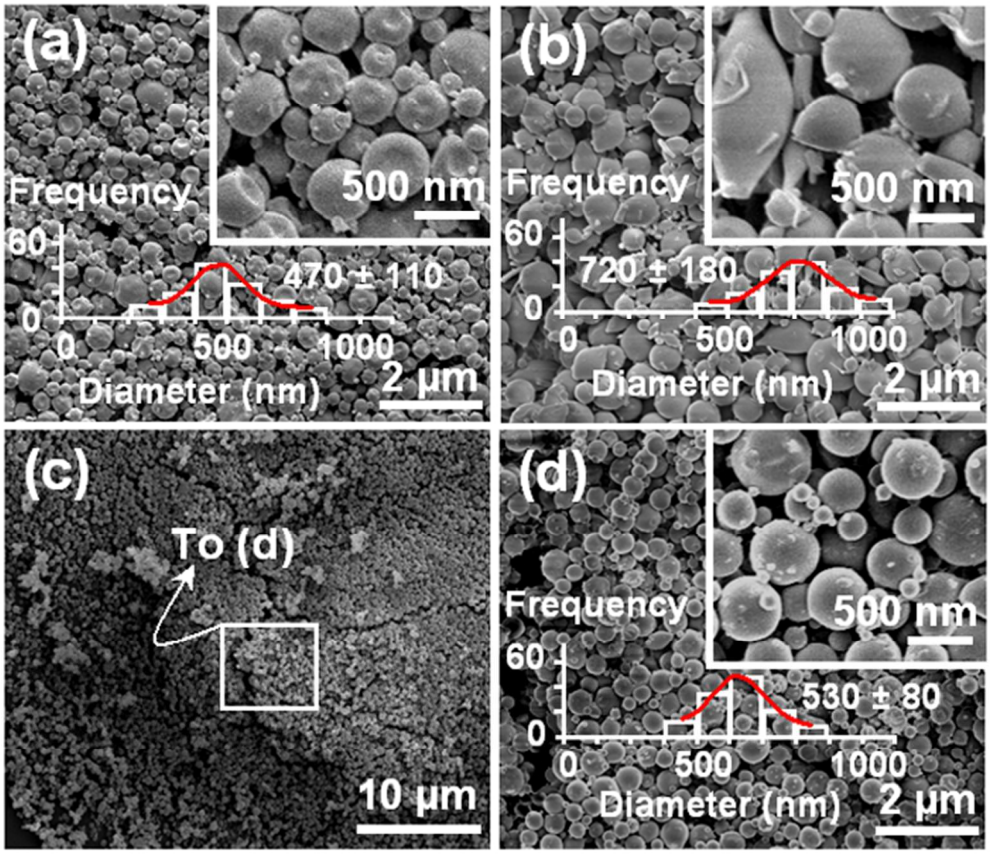

Fig. 3 FESEM images of the nanoparticles, and their diameter distributions, (a) nanoparticles N1, (b) nanoparticles N2, (c) and (d) nanoparticles N3 with different magnifications
60x51mm (300 x 300 DPI)

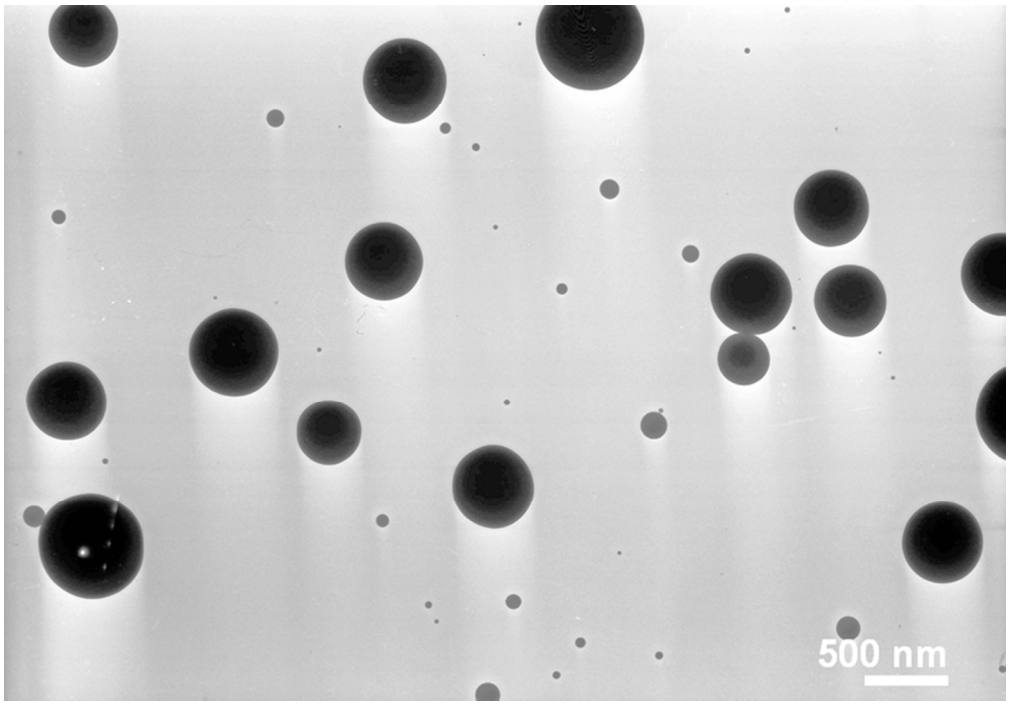

Fig. 4 TEM images of nanoparticles N3
70x48mm (300 x 300 DPI)

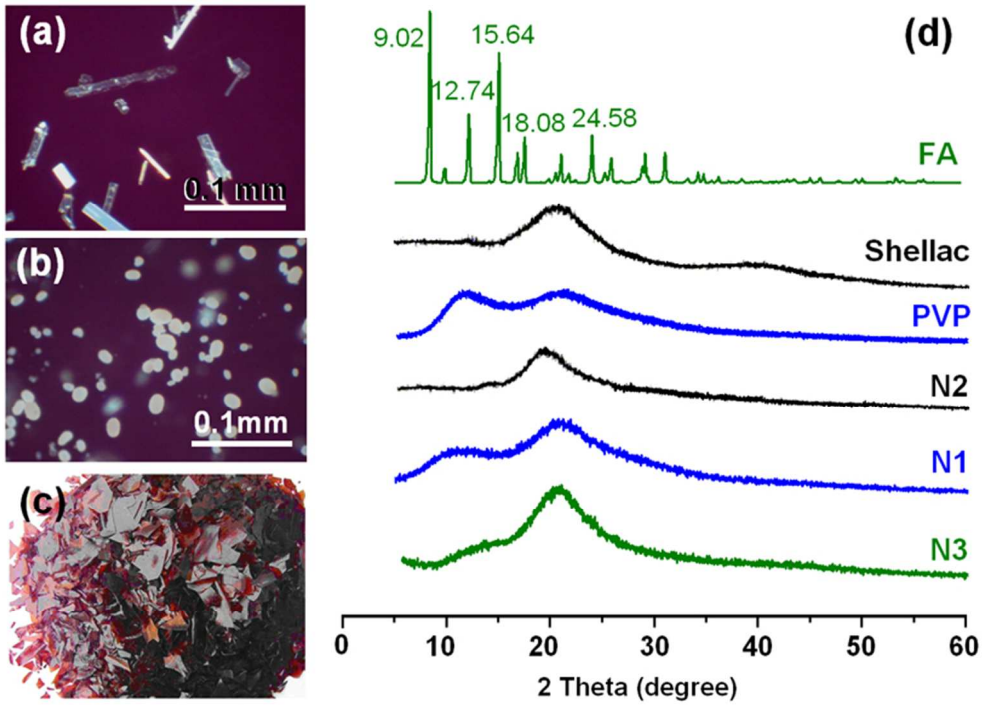

Fig. 5 XRD patterns and observations of the crude particles. a) microscopy images viewed under cross-polarized light: a) FA; b) PVP; c) a digital image of shellac; d) XRD patterns of the starting materials and nanoparticles N1, N2, and N3
70x49mm (300 x 300 DPI)

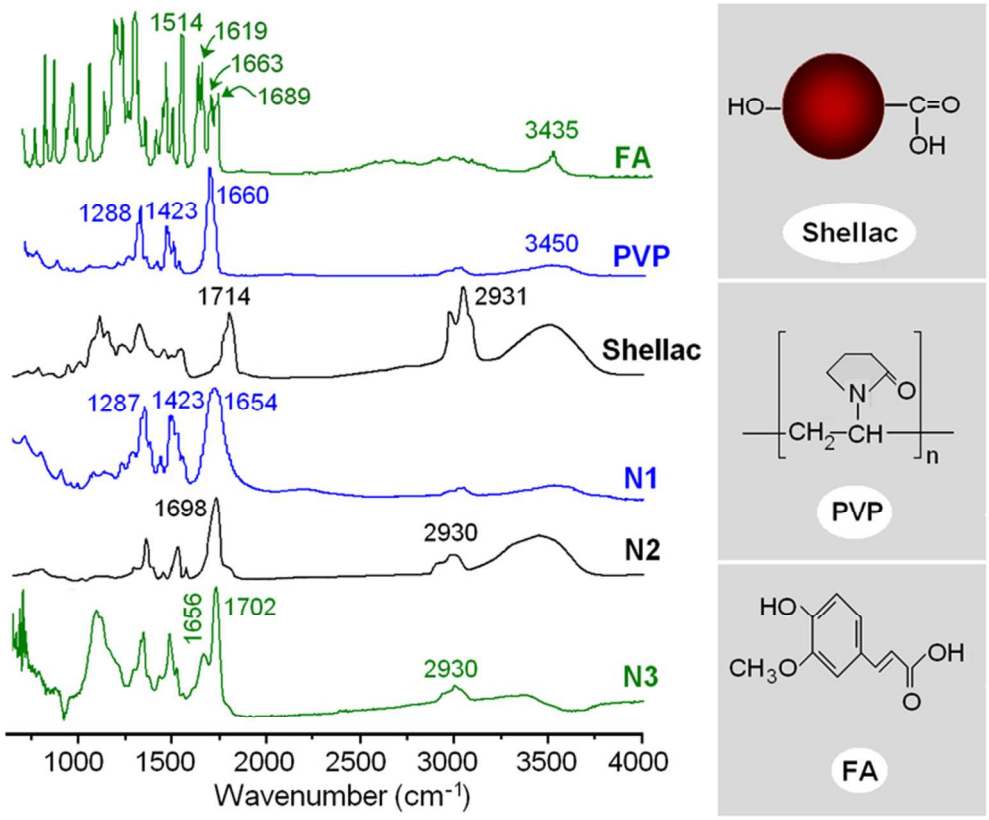

Fig. 6 ATR-FTIR spectra of the raw materials and nanoparticles, and the molecular structures of PVP, FA and shellac
70x57mm (300 x 300 DPI)

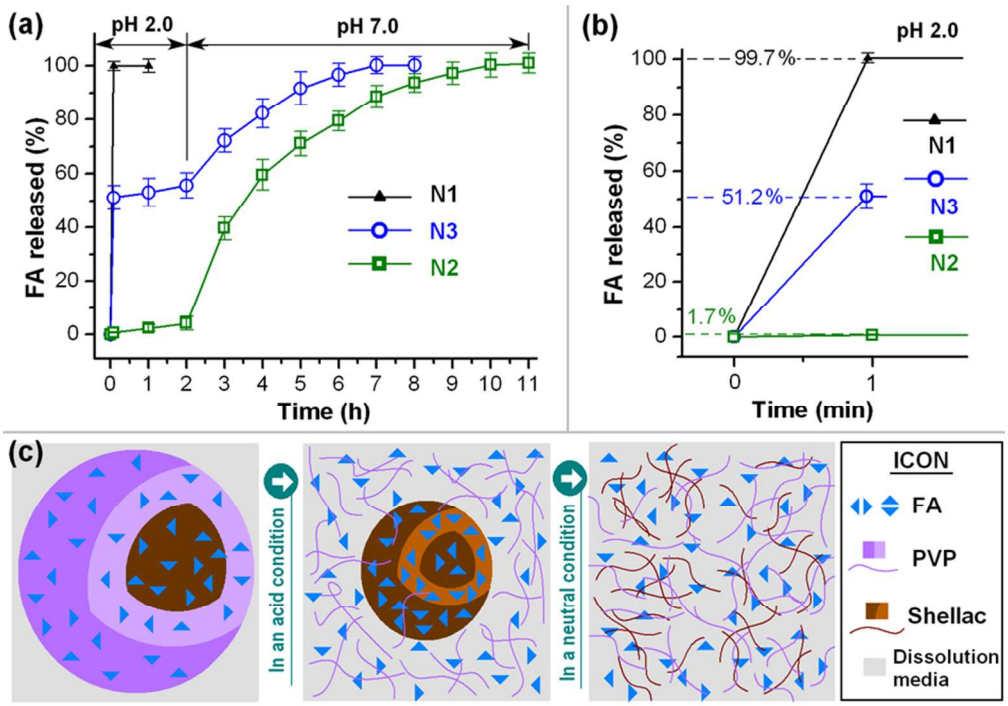

Fig. 7 In vitro dissolution tests. a) in vitro FA release profiles during the whole time period (n=6); b) in vitro FA release profiles of the first hour (n=6); c) a schematic about the drug controlled release mechanisms from the core-shell nanoparticles
80x56mm (300 x 300 DPI)